

Spatio-temporal variation of surface suspended particulate matter concentration in the Belgian-Dutch coastal zone*

Matthias Baeye¹, Michael Fettweis², Bouchra Nechad², Vera Van Lancker²

¹ Ghent University, Renard Centre of Marine Geology, Krijgslaan 281 (S8), 9000 Gent, Belgium

² Royal Belgian Institute of Natural Science, Management Unit of the North Sea Mathematical Models, Gulledele 100, 1200 Brussels, Belgium

*submitted for publication in Estuaries and Coasts (Springer)

M. Baeye handled and interpreted the datasets (SPM maps and time-series), wrote the manuscript and made all figures. Co-authors helped by reviewing the manuscript and/or providing the datasets (MODIS-SPM maps were made available by MUMM/REMSEM team). M. Fettweis carried out entropy analysis of MODIS-SPM spatial data.

Abstract

Suspended particulate matter (SPM) concentration maps, derived from satellite remote sensing (MODIS-Aqua) data, were evaluated for their use in the assessment of coastal turbidity maximum (CTM) dynamics in Belgian coastal waters. The CTM is a dynamic coastal feature of which the geographic position and extent varies under different meteorological, astronomical and climatological conditions. Analyses were based on grouping-averaging of SPM concentration maps, using different classification schemes. To better spatially depict the CTM, entropy grouping was introduced. This technique analyses, per pixel, the total information contained within the probability distribution of SPM concentration. Results revealed wind-induced variations in position and extent of the CTM, with southwesterly winds inducing a largest CTM extent, in contrast to a strong reduction under northeasterly winds. Climate-induced variations were assessed contrasting 2 winters with opposing indices of the North Atlantic Oscillation (NAO). In a winter with a positive NAO index, hence stronger-than-average southwesterly winds, the CTM was extended to the Dutch waters, whereas the opposite occurred in winters with a negative NAO index, hence less-than-average southwesterly winds. To evaluate astronomical forcing (tides) grouping-averaging was performed of SPM concentration maps over a tidal cycle, and spring-neap conditions. Although, only part of the tidal cycle can be analysed, due to the sun-synchronicity of the MODIS-Aqua satellite, comparison of the results with in-situ data from a single observatory station showed good resemblance. It is concluded that MODIS-Aqua satellite data can be used to assess SPM concentration variability related to tides, neap-spring cycles, meteorological and climatological events.

Keywords: Coastal turbidity maximum; MODIS-Aqua; wind climate; tides; entropy analysis; NAO

3.1. Introduction

Mapping of suspended particulate matter (SPM) concentration from satellite imagery has become a valuable source of data to assess and monitor SPM concentration distribution (Trisakti et al. 2005, Nechad et al., 2010). These satellite data have been used in various ways and have been combined with in-situ measurements (van Raaphorst et al. 1998, Ruhl et al. 2001, Fettweis et al., 2007), sediment transport models (Vos and Gerritsen 1997, Pleskachevsky et al. 2005, Blaas et al., 2007), or have been used in the light forcing of ecosystem models (Lacroix et al., 2007). SPM dynamics control processes such as sediment transport, deposition, re-suspension and primary production and the functioning of benthic communities (McCandliss et al. 2002, Murray et al. 2002). It varies as a function of harmonic forcings such as tides, spring-neap tidal cycles and seasons, and random events such as storms or human activities. The interaction of cohesive and non-cohesive sediments, biological activity, remote or local availability of fine sediments and advective processes further influences SPM concentration (Velegakis et al. 1997, Bass et al. 2002, Schoellhamer 2002, Le Hir et al. 2007, Fettweis et al. 2010).

The inner shelf of the Belgian coast, located in the southern North Sea, is an example of an area where bed sediment composition varies from pure sand to pure mud (Verfaillie et al. 2006). It is characterized by elevated SPM concentrations (Fettweis et al. 2010) and has been subject of high anthropogenic stresses due to harbour extension, dredging and disposal works and deepening of navigation channels (Du Four and Van Lancker 2008). Effects of various hydrodynamic forcings (tidal and wind-induced flows) on suspended sediment transport has been investigated, based on in-situ data; these indicated that a modification of the hydrodynamic forcing and thus SPM concentration results from alongshore advection, due to wind-induced flows (Baeye et al. 2011, see also Chapter 4). Such Eulerian in-situ measurements indicated that the position of the coastal turbidity maximum, and as such also the origin of SPM changed according to predominant wind directions. Variations in horizontal gradients should ideally be measured with techniques having a high geographical and temporal coverage, hitherto not or only partially available (Neukermans et al. 2009, Sirjacobs et al. 2011).

Wide swath polar-orbiting ocean colour remote sensors such as MODIS-Aqua have been used successfully to assess seasonal and intra-annual SPM concentration variability (Fettweis et al. 2007, Eleveld et al. 2008, Pietrzak et al. 2011). The long term time-series of MODIS-data for some locations in the southern North Sea reveal clearly the dominant seasonal signal (Nechad et al. 2010). However, irregular and shorter-term variations, not directly linked to seasons, can also be identified in these time-series. The aim of this paper is to investigate these random variations by linking them to typical meteorological, climatological and tidal conditions in the time and spatial domain. Such findings allow a separation and recognition of processes that control their variability and can be used for understanding the long-term evolution of the system, and potentially for prediction of future (climate-induced) changes. Further, the possible use of MODIS-Aqua imagery to assess SPM concentration variability related to tides, neap-spring cycles, and meteorological and climatological events is evaluated and compared to in-situ measurements of SPM concentration.

3.2. Environmental setting

3.2.1. Coastal turbidity maximum

The study area is located in the southern North Sea, comprising the Belgian-Dutch coastal waters and the mouth of the Westerscheldt estuary (Fig. 3.1). Water depths vary between 3 and 15 m MLLWS (Mean Lowest Low Water Spring) with shallow sand ridges, gullies and navigation channels that result in an overall complex, and irregular bathymetry (Fig. 3.1). The seabed consists of sands mainly; however, a Holocene mud plate exists between Zeebrugge and Ostend (Mathys 2009). The coastal environment is not associated with an aggradational shelf from river output; the most important sources of SPM are the erosion of nearshore Holocene and recent mud deposits, the French rivers discharging into the English Channel, and the coastal erosion of the

Cretaceous cliffs at Cap Gris-Nez and Cap Blanc-Nez (France) (Fettweis et al. 2007, Zeelmaekers 2011). The Westerscheldt estuary is considered a storage for mud, rather than a source of SPM (Van Maldegem et al. 1993, Verlaan et al. 1998, see also Chapter 2). Cohesive sediments are trapped in the coastal turbidity maximum (CTM), due to tidal forcing and flocculation of SPM. Hydrodynamic and meteorological forcings cause a congestion of the residual transport in the area. Elongated tidal ellipses, with strong tidal currents and relatively long slack waters (about 1 hour), stimulate flocculation and break-up and thus settling and re-suspension of fine-grained material.

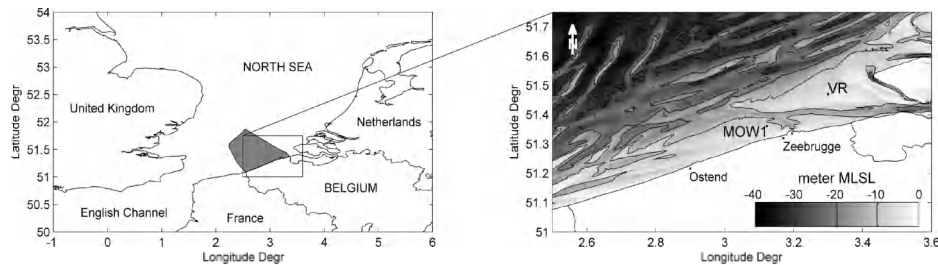


Figure 3.1 Study area location in the southern Bight of the North Sea (**left**). Depths (every 10 m) in meters Mean Low Sea Level, and the location of the *in-situ* observatory station (MOW1) and the Westerscheldt estuary mouth (VR) (**right**)

The astronomical tides are semi-diurnal with an average range of 4.3 m (2.8 m) at spring (neap) tide at Zeebrugge. Overall, residual water transport is from southwest to northeast. Further, the complex, irregular bathymetry, together with the freshwater discharges, also influences the mean circulation, the residual transport field and the spreading of the freshwater in the coastal zone (Arndt et al., 2011). Strong tidal currents (up to 1 m.s^{-1}) lead to a relatively well-mixed water column in the coastal zone, with salinity varying between 28 and 34, due to wind-induced advection of water masses and river discharges (Yang 1998, Lacroix et al. 2004).

3.2.2. Weather and climate

The continental coasts in the southern North Sea are subjected to a large scale west to east circulation of depressions, and to the development or weakening of high pressure systems. These fluctuations of the wind field occur at time scales of a few days to one week (Wieringa and Rijkort 1983, Delhez and Carabin 2001). Onshore NW winds are associated with mid-latitude low-pressure systems causing high sea surges, mainly during winter periods (Ulman and Monbaliu 2010). Southwesterly winds dominate the wind regime for the decade 2001-2010, followed by northeasterly winds (Fig. 3.2 a). An increase in the frequency of west-southwesterly winds over the last decades is observed (Siegmund and Schrum 2001, Van den Eynde et al. 2011). On a global scale, the North Atlantic Oscillation (NAO) is responsible for much of the observed weather and climate variability, especially during winter months (December through March) (Hurrell 1995, Hurrell and Deser 2009). This wintertime NAO exhibits significant multi-decadal variability with positive values indicating anomalously strong westerly winds and wet conditions over northwestern Europe, whereas negative values exhibit weaker westerly flow and less precipitation (Hurrell 1995, Chelliah and Bell 2004).

3.3. Methodology

3.3.1. MODIS SPM concentration

The Moderate Resolution Imaging Spectro-radiometer (MODIS) onboard the Aqua satellite, part of the NASA Earth Observation System (EOS), provides 1 to 2 daily images over the North Sea area. These data are used to build up daily maps of SPM concentration. 2539 MODIS images, covering 9 year between July 2002 and December 2009, have been processed from Level 1A (NASA/Ocean Biology Processing Group

website, <http://oceancolor.gsfc.nasa.gov/cgi/browse.pl?sen=am>) to Level 2, using the SeaDAS software (available at <http://oceancolor.gsfc.nasa.gov/seadas/>). This consists of 2 steps: producing the Level 1B data by geo-referencing Level 1A data, and subtracting the atmospheric contributions by air molecules and aerosols from the radiances measured by the sensor at the top of the atmosphere; these yield the L2 data, where marine reflectances, ρ_w (" w " referring to water), at MODIS bands may be obtained. Surface SPM concentration (further referred to as "SPM concentration") is then retrieved from Rrs (remote sensing reflectance) at MODIS central band wavelength 667 nm, using the algorithm of Nechad et al. (2010): $SPM = 362.1 * \rho_w / (1 - \rho_w / 0.17)$. Finally, Level 2 processing flags (Patt et al. 2003) are used to mask out the land and cloud pixels and any bad quality pixel (e.g. due to atmospheric correction failure, negative reflectance neighbouring clouds, adjacency effects).

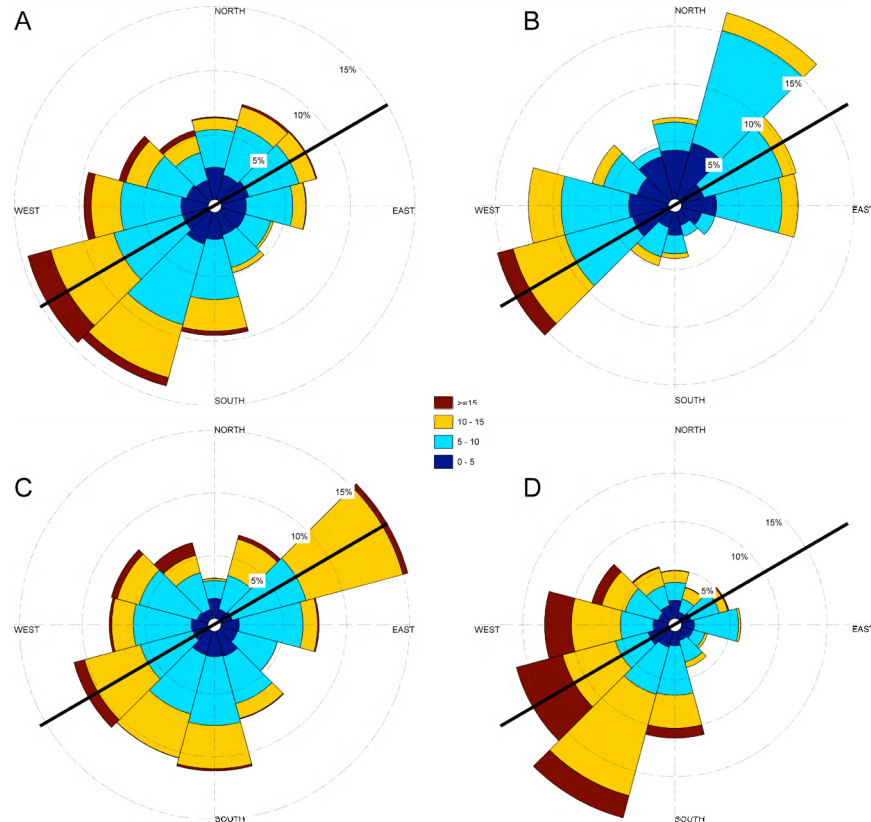


Figure 3.2 **a** Wind rose diagrams (meteorological convention "wind blowing from") with coastline orientation for the period 2001-2010. **b** Idem, for MODIS-Aqua cloud-free data images, at time of satellite overpass. **c** Idem, for negative NAO winter 2005/6 and **d** for positive NAO winter 2006/7. Wind speed in $m s^{-1}$

3.3.2. Classification and statistics of SPM concentration maps

To assess tidal, neap-spring cycles, meteorological and climatological effects on SPM concentration, different classification of SPM concentration maps have been carried out. The 2539 MODIS SPM concentration maps have been classified according to neap and spring tide, and each map was assigned to its corresponding intra-tidal phase, based on the time of MODIS-Aqua overpass (12:00-13:00 GMT). This was achieved through 3 steps:

- The tidal cycles were equally divided in 12 time intervals (~1 hour interval),
- Each tidal cycle was classified as neap or spring, based on the mean tidal range at Zeebrugge (3.6 m).

Cycles with tidal range greater than the mean range are classified as spring tides, whereas cycles with range less than 3.6 m are considered as neap tides. The SPM concentration maps were assigned neap or spring maps, based on the corresponding tidal cycles. Therefore, this classification scheme has resulted in 24 categories of SPM concentration maps, where each category represents both the semi-diurnal and fortnight tidal forcing. Per category, all maps were averaged to create a representative SPM concentration map for each case.

Meteorological effects have been addressed by classifying the satellite maps according to the wind regime, recorded at the meteorological station at Zeebrugge at the moment of MODIS-Aqua overpass. This classification was performed following four wind sectors which were defined, based on the overall wind climate measured over a decade (Fig. 3.2 a):

- a. sector around SSW is the most abundant wind sector (here after referred to as SSW case),
- b. the second wind sector comprises winds blowing from the NNE (NNE case),
- c. the third wind sector encompasses winds from mainly the WNW (WNW case),
- d. and finally land winds being the less abundant (ESE case).

Further, climatological impact has been investigated using the North Atlantic Oscillation (NAO) indices for winter SPM concentration maps. The NAO Index Data were provided by the Climate Analysis Section, NCAR, Boulder, USA, Hurrell (1995). The NAOWI (December through March) time-series exhibits two consecutive winters with opposite NAOWI index within the period of MODIS-Aqua data collection: -1.09 in winter 2005/6; and 2.79 in winter 2006/7.

For each ensemble of SPM concentration maps, an average SPM concentration map was obtained. As a result, the coastal turbidity maximum and its position along the coast are evaluated, based on the highest SPM concentration occurrences. More enhanced statistical approaches were introduced by means of entropy analysis, allowing better spatial characterization of the turbidity maximum. Entropy analysis is a statistically robust technique for grouping geographic data (Johnston and Semple 1983). Here, entropy groupings are used to categorize surface SPM concentration data ensembles (wind and NAO winter cases), taking into account the total information contained within the probability distribution curve of SPM concentration at every pixel (at which at least 100 data points exist; if not pixel is left blank). This analysis was carried out with the routine of Johnston and Semple (1983). Seven entropy groups of minimum relative entropy are used to characterize SPM concentration distribution for the entire study area; entropy groups 1 to 5 are distributions that are skewed towards lower concentrations, group 6 is intermediate, and the 7th entropy grouping (with highest median SPM concentration, and a rather normal distribution) defines the geographical extension of the coastal turbidity maximum (see 3.4.1). The entropy analysis defines the CTM area based on statistical properties rather than on absolute values; this allows comparing the geographical extension of the CTM for different wind or climatological situations.

3.3.3. In-situ SPM measurements

SPM concentration distribution in the water column was measured, in-situ, with Optical Backscatter Sensors (OBS), mounted on a water sampler and CTD (conductivity, temperature, depth) frame and on a benthic tripod. The latter was deployed in water depths of 9 m MLLWS at MOW1 station (Fig. 3.1, right). Time-series of SPM concentration were recorded at 2 m (OBS-SPM1) above the seabed (mab) for a total of ~260 days. At the MOW1 location, 16 ship-borne measurements (e.g. water and CTD profiling) were carried out during 1 tidal cycle (about 13 h). Water samples were filtered and residues were weighted in order to calibrate the OBS's of both the benthic and the CTD frame (OBS-SPM2). In-situ SPM concentrations were grouped similarly as the satellite images: per tidal phase and per spring or neap cycle. These were compared with the tidal phase averaged surface SPM concentrations, derived from MODIS at the measuring station MOW1.

3.4. Results

3.4.1. Average SPM concentration

In Fig. 3.3 a, an average SPM concentration map, based on all SPM concentration images, showed a CTM between Zeebrugge and Ostend with a maximum SPM concentration of about 50 mg l^{-1} . Offshore, SPM concentrations were reduced ($<10 \text{ mg l}^{-1}$). The entropy CTM group (7, black coloured region in Fig. 3.3 b) defined the CTM as an area that stretches from Ostend to the Dutch-Belgian border (about 40 km), with a median SPM concentration of 33 mg l^{-1} (Table 3.1); the corresponding probability distribution of the SPM concentration was normally distributed, unlike the other groups (Fig. 3.3 c). Probability distributions of SPM concentration for the 6 other groups were skewed towards the smaller SPM concentrations.

Only 20% of all SPM concentration maps corresponded with cloud-free conditions at MOW1 pixel. The wind under these conditions (Fig. 3.2 b) was compared to the overall wind rose over the last decade (Fig. 3.2 a) showing globally weaker winds, with more NE and less NW and SSW winds. Therefore, the average surface SPM concentration map (based on all SPM concentration images) is more biased towards this weather regime.

3.4.2. Average surface SPM concentration under different meteorological forcings

SPM concentration maps for the 4 wind cases (SSW, NNE, WNW and ESE) had different spatial extensions of the CTM (Fig. 3.4). SSW wind case corresponded with the largest CTM, including the mouth of the Westerscheldt estuary. This contrasted to the NNE wind case where the coastal turbidity maximum was reduced to a small area between Zeebrugge and Ostend. The ESE wind case corresponded with a maximal alongshore extent of the CTM towards France. Median SPM concentrations of entropy group 7, for each wind case, are given in Table 3.1; they indicate that SPM concentration in the CTM is the lowest for wind case WNW.

Table 3.1 SPM concentrations (mg l^{-1}) for the entropy group 7 (CTM), for each case

CASE	MEDIAN SPM mg l^{-1}
ALL	33
SSW	29
WNW	25
NNE	31
ESE	32
NAOWI ⁻	43
NAOWI ⁺	35

3.4.3. Average surface SPM concentration for contrasting winter situations

The winter of 2006/7 (NAOWI⁺) corresponded to significant SW winds, whereas the winter of 2005/6 (NAOWI⁻) was characterized by abundant NE winds (Fig. 3.2 c, d). This is reflected in the geographical distribution of the CTM shown in the associated SPM concentration, and entropy grouping maps (Fig. 3.5). The CTM during positive NAO winter conditions had shifted significantly towards the NE and was absent in front of Ostend. A negative NAO winter coincided with a CTM extending over nearly all the Belgian coast, up to the mouth of the Westerscheldt. Median SPM concentrations during NAOWI⁻ were higher (43 mg l^{-1}) than during NAOWI⁺ (35 mg l^{-1}) (Table 3.1).

3.4.4. Average surface SPM concentration for different hydrodynamic conditions

The influence of tides and neap-spring cycles on surface SPM concentration is shown in Fig. 3.6. Remark that during neap and spring tide only 7 of the 12 cases are represented. Data are centered around low water (LW) during neap tide and around high water (HW) during spring tide. SPM concentration was generally higher during

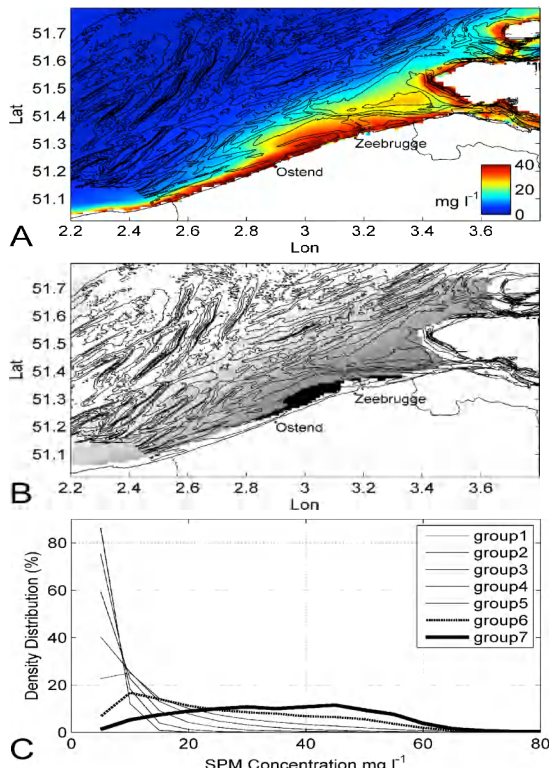


Figure 3.3 *a* Surface SPM map, as an average of all MODIS-Aqua data images. *b* Surface SPM map, obtained from entropy analysis grouping SPM concentrations in 7 classes. Black coloured class (group 7) corresponds to the actual CTM and *c* Corresponding probability distribution curves of SPM concentration

spring tide than neap tide. Highest SPM concentrations occurred at 4 hours before HW (HW-4, i.e. 2-3 hours after LW). During flood the CTM shifted towards the mouth of the Westerscheldt estuary.

The tide-induced variation in the MODIS images has been compared with in-situ data at MOW1, measured at 2 meters above bottom (mab) and near the surface (Fig. 3.7 a, c). A tidal ellipse at MOW1 (Fig. 3.7 b, d) shows that maximum ebb and flood currents occurred at LW and HW, respectively. A peak in SPM concentration at 2 mab occurred around HW and LW, with the highest SPM concentration (600 mg l^{-1}) around LW. Lowest SPM concentrations at 2 mab (100 mg l^{-1}) were observed around slack water (HW-3 and HW+3). Surface maxima and minima in SPM concentration (in-situ and MODIS) occurred later than the maxima and minima at 2 mab, due to a settling and re-suspension time lag. Although the MODIS SPM concentration curves were incomplete for both neap and spring conditions, in-situ minima/maxima in SPM concentration correlated well with near-surface data.

3.5. Discussion

3.5.1. Evaluation of the use of MODIS

Satellite data reveal variations in surface SPM concentration in the CTM resulting from tidal, neap-spring tidal cycle, meteorological and climatological forcings. The most pronounced cycle is related to seasonal variations and is well described in literature (Fettweis et al. 2007, Van den Eynde et al. 2007, Pietrzak et al. 2011). Winter SPM concentrations are a factor 2 higher than summer concentrations; although SPM concentration can vary during different winter periods, depending on climatological conditions. Influences of spring-neap cycles are clearly identified in both the in-situ

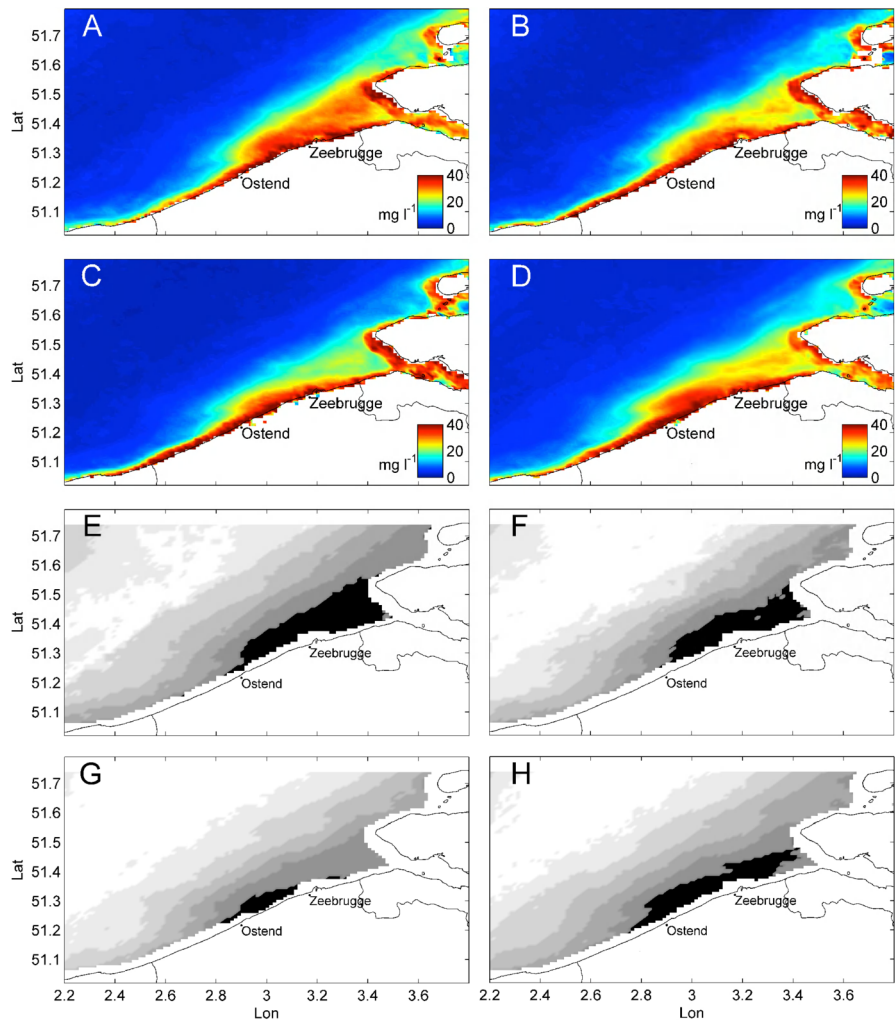


Figure 3.4 Representative surface SPM concentration maps for the wind cases obtained from grouping-averaging MODIS-Aqua data images: SSW (**A**), WNW (**B**), NNE (**C**), ESE (**D**). Entropy grouping maps for the wind cases: SSW (**E**), WNW (**F**), NNE (**G**), ESE (**H**)

data (Chapter 2; Baeye et al. 2011), and MODIS data. SPM concentration measured at the surface corresponds to events of re-suspension, mixing, settling and deposition. For the relative shallow MOW1 location, a time lag of about 1 hour was identified between maximum SPM concentration near the bed (in-situ data) and at the surface (satellite), which corresponds well with literature (Bass et al. 2002). In deeper water the time lag is longer, which is also reflected in the general lower surface SPM concentration in the deeper areas, such as the navigation channel towards the Westerscheldt, situated in the CTM.

MODIS-Aqua cannot be used to gather data during a whole tidal cycle for spring and neap tides (Doxaran et al. 2009, van der Wal et al. 2010). This is a result of the 24 h sampling interval of the MODIS-Aqua which is 0.84 h shorter than the 24.84 h period of the diurnal tide. Every 15 days the same phase of the tide is sampled, corresponding to the periodicity of the spring – neap cycles. As a result, parts of the tidal cycle in relation to spring-neap tides are not captured by sun-synchronous satellites, such as MODIS-Aqua. Therefore, when grouping SPM concentration maps (per season, per wind case, per month etc.) followed by ensemble-averaging, the resulting SPM concentration maps inherently incorporate under-sampling. In-situ data

show that SPM concentration is highest during LW at spring tides; a tidal phase that is never measured by MODIS-Aqua in the study area. The latter, together with the fact that satellite images consist of a subset of the population, biased towards good weather condition or spring-summer seasons (Fettweis and Nechad 2011), explain also the lower SPM concentrations found in the satellite images when comparing to in-situ data. Surface sediment transport or light infiltration in turbid waters, based on these data, will thus always underestimate reality.

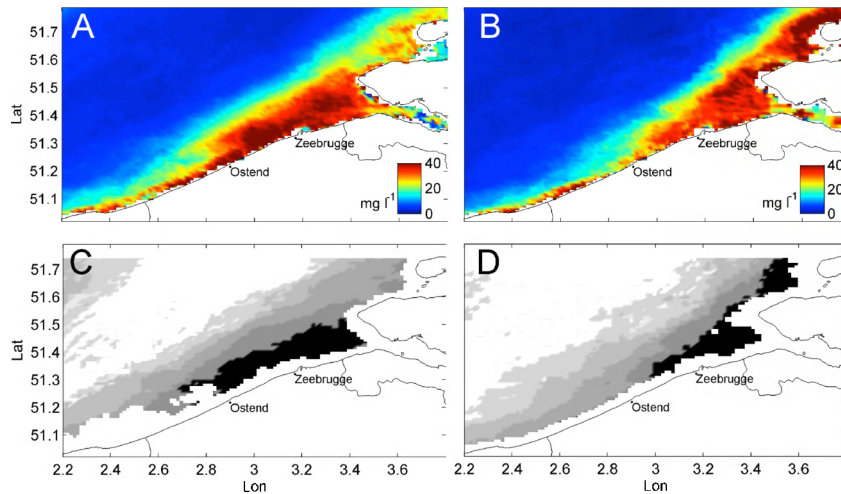


Figure 3.5 Representative surface SPM concentration maps for two contrasting winters: NAOWI- (2005/6) (**A**) and NAOWI+ (2006/7) (**B**) and the corresponding entropy grouping maps (**C**) and (**D**), respectively

3.5.2. Wind-induced CTM dynamics

Variability of SPM concentration is evaluated using the coefficient of variations (CV), which is calculated from the ratio of the standard deviation of SPM divided by SPM concentration (Fig. 3.8 a). Lower CV is associated to areas with a rather low relative SPM concentration variability, such as the CTM zone. Two areas can be identified: one with a slightly higher CV, corresponding to the mouth of the Westerscheldt and the Vlakte van de Raan and the other with slightly lower CV situated between Ostend and Zeebrugge. The latter area shows high SPM concentrations more often than the former area. This was already pointed out by Nechad et al. (2003) and Van den Eynde et al. (2007); however, without providing a convincing explanation. Current analyses relate this different behaviour to wind-induced alongshore advection of the CTM zone. For instance, the area of the mouth of the Westerscheldt estuary and the Vlakte van de Raan has, e.g. lower SPM concentrations during NE-E wind conditions (Fig. 3.4 c, g). Fig. 3.3 shows also that the area between Ostend and Zeebrugge has high SPM concentrations during all wind conditions. The role of alongshore advection of water masses has been investigated, based on near-bed in-situ data from a station near Zeebrugge (Baeye et al., 2011). Data have shown that winds blowing from the SW are inducing a subtidal alongshore flow towards the NE bringing less turbid and more saline waters originating from the Strait of Dover towards the CTM. Higher SPM concentration waters are extending more towards the NE up to the mouth of the Westerscheldt (Fig. 3.4 a, f). Prevailing NE winds reverse the subtidal alongshore flow resulting in a decrease of salinity near Zeebrugge, due to an enhanced outflow of the Scheldt estuary (Arndt et al. 2011). The latter is associated with an increase of SPM concentration near Zeebrugge and the formation of high concentrated mud suspensions (HCMS) near the bed (Baeye et al. 2011). This is in contrast with the satellite images, which have on average lower surface SPM concentrations in the area between Zeebrugge and the mouth of the Westerscheldt under NNE winds. Differences between remote sensing and in-situ datasets underline that near bed SPM concentration dynamics is partially uncoupled from processes higher up in the water

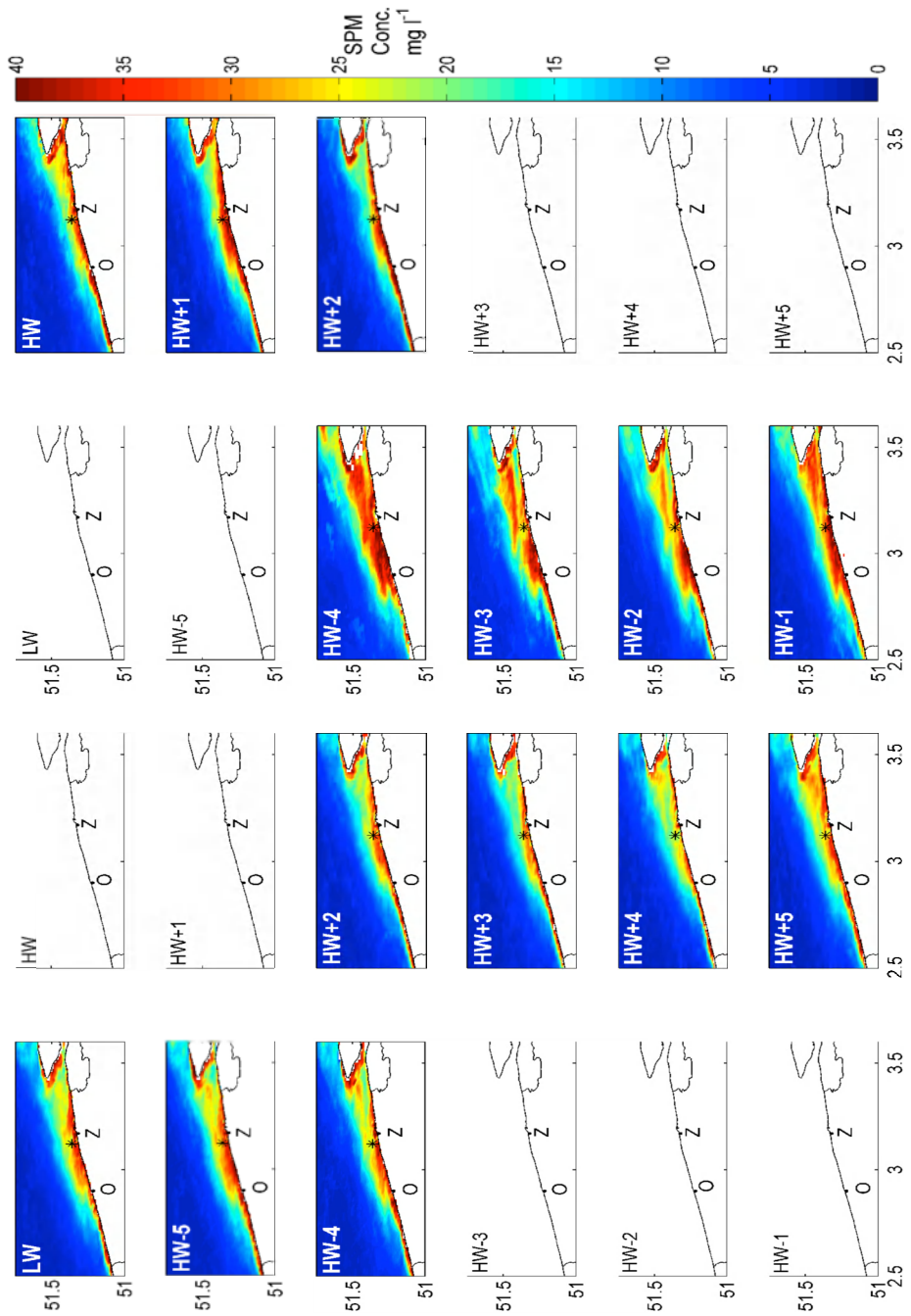


Figure 3.6 Surface SPM concentration maps for intra-tidal phases (phase interval of about 1 hour) for neap (**left**) and spring (**right**) tidal conditions. Phases with blank maps correspond with no or not enough data. Consequently, low water phases of MODIS imagery occur only under neap tide; high water phases only during spring tide

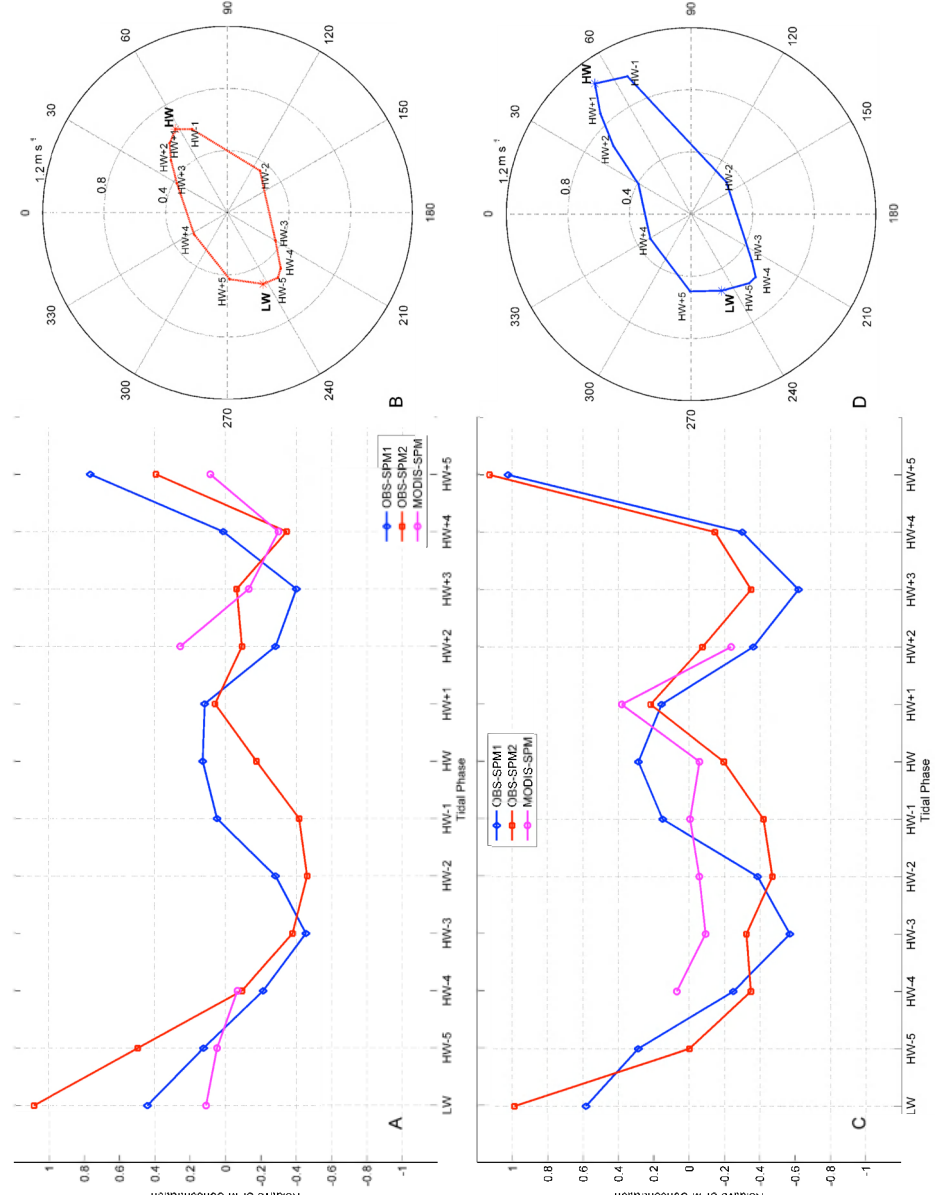


Figure 3.7 Relative SPM concentration per intra-tidal phase from in-situ (MOW1 station) measurements (at 2 m above bed (SPM-OBS1), near surface (SPM OBS2)) for neap (**A**) and spring (**C**) tidal conditions, together with MODIS-Aqua intra-tidal phase averages at MOW1. Tidal ellipse representative for the coastal zone between Ostend and Zeebrugge for neap tide (**B**) and spring tide (**D**) conditions

column (Fettweis and Nechad 2011).

The CTM for the ESE wind case is slightly more extended towards France, which is caused by a strong subtidal alongshore flow towards the SW and an enhanced outflow of the Westerscheldt estuary. The CTM entropy class 7 is not connected with the Westerscheldt estuary (Fig. 3.4 d, h) confirming earlier studies that considered the estuary as not an important source of SPM (Van Maldegem et al. 1993, Verlaan et al. 1998). Further, the ESE and the WNW wind cases generate cross-shore winds inducing coastal set-up and set-down, respectively. This will change the overall water depth and consequently the overall SPM concentrations in the coastal zone (e.g. Hommersom et

al. 2010). The higher median SPM concentrations for entropy class 7 under ESE winds, and the lower median SPM concentration associated with the NW winds (WNW wind case) is thus possibly also influenced by coastal set-down (-0.5 m) and set-up (+0.5 m), respectively.

The grouping-averaging of SPM concentration images per wind case is seasonally biased as winds are not equally distributed during a year (Jones et al. 1994). Wind climates per season, based on local wind field data during MODIS overpass, show that: (1) wind case SSW is well-represented throughout the year; (2) wind case N-NE is representative for all seasons, except for winter; and (3) NNW and ESE wind cases are more abundant during winter and autumn, than during summer and spring. A simple averaging of all MODIS images (Fig. 3.2 a) is therefore not a good representation of an average SPM concentration. In Fig. 3.8 (b) an unbiased averaging was carried out, based on the weighted averages of the different wind cases (percentage of occurrence and linear scale). Comparison between Fig. 3.3 (a) and Fig. 3.8 (b) shows that the CTM is more positioned towards the Westerscheldt estuary mouth (Fig. 3.8 c).

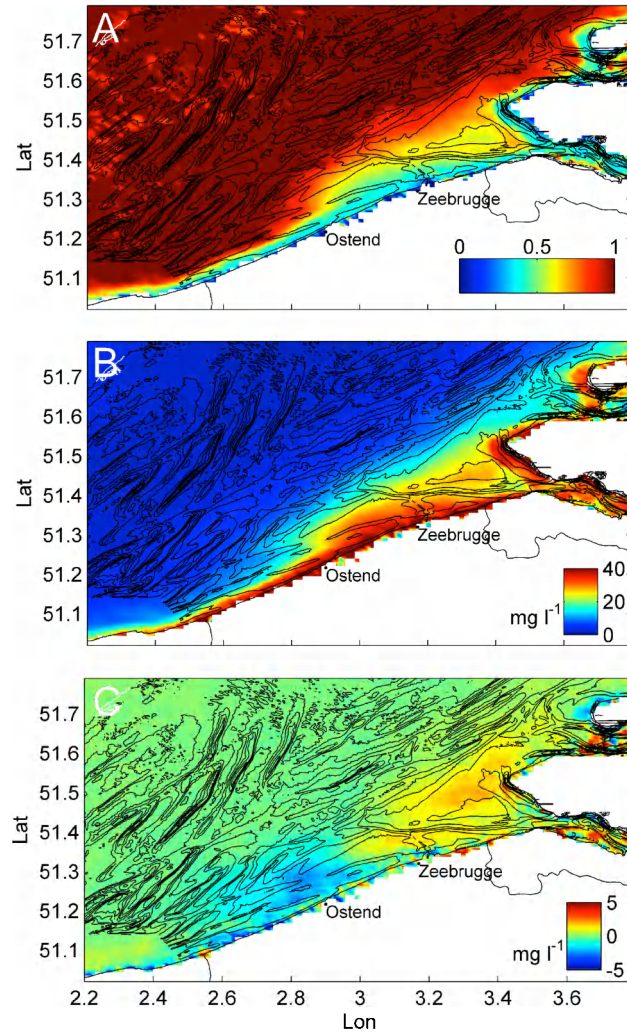


Figure 3.8 Map of coefficient of variation (standard deviation map divided by average map) with "0" referring to low surface SPM variability, and "1" to high variability, based on all MODIS-Aqua images (**A**). Unbiased average surface SPM map based on the weighted averages of the different wind cases (**B**). Map of difference in surface SPM between A and B (**C**)

3.5.3. Weather, climate and environmental changes

Changes in weather patterns affect the coastal hydrodynamics, and consequently the sediment transport of fine-grained, cohesive sediments. The influence of contrasting NAO conditions during two winters has a striking effect on the spatial extension of the CTM zone (Fig. 3.5). Over the last decades, trend analysis of wind directions shows an increase of southwesterly winds (Siegismund and Schrum 2001, Van den Eynde et al. 2011). The geographical extension of the CTM during the last decades was thus more often spreading towards the mouth of the Westerscheldt estuary as before, similarly to wind case SSW (Fig. 3.4). Houziaux et al. (2011) formulated similar remarks, based on a comparison of historical (100 year) and recent bed samples. These authors have related the changes to mainly port and dredging works that have severely altered the fine-grained sediment dynamics; hence also the turbidity levels in the coastal zone. Our data suggest that the spatial extension of the CTM, and thus SPM concentration is further influenced by natural changes.

The consequences of variations in spatial extension of the CTM zone which has occurred during the last decades must now be completed with specific analyses, e.g. have changes in macrobenthic species communities occurred since they are influenced by SPM availability, as SPM carries a major part of the food resources for the benthos; however, it might turn into an environmental stressor when SPM concentrations interfere with species filtering and respiratory systems (Rodriguez-Palma 2011). As a result, changes in benthos will likely reflect both the natural and anthropogenic disturbances in coastal environments (Dauer et al. 2000, Dauvin et al. 2007).

3.6. Conclusions

The coastal turbidity maximum along the Belgian-Dutch coast is not a static feature. The seasonality in the SPM concentration map time-series is superimposed by SPM concentration variations acting on shorter time scales. The paper addresses the variations that are induced mainly by meteorological forcing. Wind direction plays a significant role in the position and extent of the CTM, as observed at the sea surface. Wind field fluctuations occur over several days and as a consequence, the residual transport of fine sediments will vary, as well as the position of the CTM. Southwesterly winds typically correspond to a largest spatial extent of the CTM, whereas northeasterly winds impose a reduction. More significant alongshore displacement in CTM position towards the Dutch coastal waters is seen in winter months with stronger-than-average southwesterly winds. Winter periods also exist in which SW winds are less abundant, resulting in different CTM spatial patterns. The latter is based on the climatological index, North Atlantic Oscillation, even substantially influencing CTM position for longer periods (4 months). Astronomical forcing (tides) was evaluated also. The group-averaged, intra-tidal SPM concentration maps showed good similarities with in-situ data. It is concluded that MODIS-Aqua satellite data can be used to assess SPM concentration variability related to tides, neap-spring cycles, and meteorological and climatological events.

3.7. Acknowledgements

The study was partly funded by Belgian Science Policy (Science for a Sustainable Development, QUEST4D, SD/NS/06A; STEREO programme; Belcolour-2 project, SR/00/104) and partly by the Maritime Access Division of the Flemish Authorities (MOMO project). G. Dumon (Flemish Authorities, Maritime Services, Coastal Division/Hydrography) made available wind data. We want to acknowledge the crew of RV Belgica, Zeearend and Zeehond for their skilful mooring and recuperation of the tripod. Measurements would not have been possible without technical assistance of A. Pollentier, J.-P. De Blauwe and J. Backers (Measuring Service of MUMM, Oostende). The first author acknowledges a specialisation grant from IWT (Agency for Innovation by Science and Technology, Flanders).

3.8. References

- Arndt S, Lacroix G, Gypens N, Regnier P, Lancelot C (2011). Nutrient dynamics and phytoplankton development along an estuary-coastal zone continuum: A model study. *Journal of Marine Systems* 84 (3-4), 49-66.
- Baeye M, Fettweis M, Voulgaris G, Van Lancker V (2011). Sediment mobility in response to tidal and wind- driven flows along the Belgian inner shelf, southern North Sea. *Ocean Dynamics* 61(5), 611-622.
- Bass SJ, Aldridge JN, McCave IN, Vincent CE (2002). Phase relationships between fine sediment suspensions and tidal currents in coastal seas. *Journal of Geophysical Research* 107(C10), 1-14.
- Blaas M, El Serafy GYH, van Kessel T, de Boer GJ, Eleveld MA, van der Woerd HJ (2007). Data model integration of SPM transport in the Dutch coastal zone. *Proceedings of the Joint 2007 EUMETSAT/AMS Conference*, 1–8.
- Chelliah M, Bell GD (2004). Tropical multi-decadal and interannual climate variations in the NCEP/ NCAR Reanalysis. *Journal of Climate* 17, 1777-1803.
- Dauer DM, Ranasinhe JA, Weisberg SB (2000). Relationships between benthic community condition, water quality, sediment quality, nutrient loads, and land use patterns in Chesapeake Bay. *Estuaries* 23, 80-96.
- Dauvin J-C, Ruellet T, Thiebaut E, Gentil F, Desroy N, Janson A-L, Duhamel S, Jourde J, Simon S (2007). The presence of *Melinna palmata* (Annelida: Polychaeta) and *Ensis directus* (Mollusca: Bivalvia) related to sedimentary changes in the Bay of Seine (English Channel, France). *Cahiers Biologie Marine* 48, 391-401.
- Delhez EJM, Carabin G (2001). Integrated modeling of the Belgian coastal zone. *Estuarine, coastal and shelf science* 53(4), 477-491.
- Doxaran D, Froidefond JM, Castaing P, Babin M (2009). Dynamics of the turbidity maximum zone in a macrotidal estuary (the Gironde, France): observations from field and MODIS satellite data. *Estuarine, Coastal and Shelf Science* 81, 321–332.
- Du Four I, Van Lancker V (2008). Changes of sedimentological patterns and morphological features due to the disposal of dredge spoil and the regeneration after cessation of the disposal activities. *Marine Geology* 255(1-2), 15-29.
- Eleveld MA, Pasterkamp R, van der Woerd HJ, Pietrzak JD (2008). Remotely sensed seasonality in the spatial distribution of sea-surface suspended particulate matter in the southern North Sea. *Estuarine, Coastal and Shelf Science* 80, 103-113.
- Fettweis M, Nechad B, Van den Eynde D (2007). An estimate of the suspended particulate matter (SPM) transport in the southern North Sea using SeaWiFS images, in-situ measurements and numerical model results. *Continental Shelf Research* 27, 1568-1583.
- Fettweis M, Francken F, Van den Eynde D, Verwaest T, Janssens J, Van Lancker V (2010). Storm influence on SPM concentrations in a coastal turbidity maximum area with high anthropogenic impact (southern North Sea). *Continental Shelf Research* 30, 1417-1427.
- Fettweis M, Nechad B (2011). Evaluation of in-situ and remote sensing sampling methods for SPM concentrations, Belgian continental shelf (southern North Sea). *Ocean Dynamics* 61, 157-171.
- Fettweis M, Baeye M, Francken F, Lauwaert B, Van den Eynde D, Van Lancker V, Martens C, Michielsen T (2011). Monitoring the effects of disposal of fine sediments from maintenance dredging on suspended particulate matter concentration in the Belgian nearshore area (southern North Sea). *Marine Pollution Bulletin* 62, 258-269.
- Hommersom A, Wernad MR, Peters S, de Boer J (2010). A review on substance and processes relevant for optical remote sensing of extremely turbid marine areas, with a focus on the Wadden Sea. *Helgoland Marine Research* 64, 75-92.
- Houziaux J-S, Fettweis M, Francken F, Van Lancker V (2011). Historic (1900) seafloor composition in the Belgian-Dutch part of the North Sea: A reconstruction based on calibrated visual sediment descriptions. *Continental Shelf Research* 31(10), 1043-1056.

- Hurrell JW (1995). Decadal Trends in the North Atlantic Oscillation: Regional Temperatures and Precipitation. *Science* 269, 676-679.
- Hurrell JW, Deser C (2009). North Atlantic climate variability: The role of the North Atlantic Oscillation. *Journal of Marine Systems* 78(1), 28-41.
- Johnston RJ, Semple RK (1983). Classification using information statistics: Concepts and techniques in Modern Geography 46. Geobooks, Norwich, 157-160.
- Jones SE, Jago CF, Prandtl D, Flatt D (1994). Suspended sediment dynamics: measurements and modelling in the Dover Strait. In: Beven, K.J., Chatwin, P.C., Milbank, J.H. (Eds.), *Mixing and transport in the environment*. Wiley, 183-201.
- Lacroix G, Ruddick K, Ozer J, Lancelot C (2004). Modelling the impact of the Scheldt and Rhine/Meuse plumes on the salinity distribution in Belgian waters (southern North Sea). *Journal of Sea Research* 52(3), 149-163.
- Lacroix G, Ruddick K, Park Y, Gypens N, Lancelot C (2007). Validation of the 3D biogeochemical model MIRO&CO with field nutrient and phytoplankton data and MERIS-derived surface chlorophyll a images. *Journal of Marine Systems* 64, 66-88.
- Le Hir P, Monbet Y, Orvain F (2007). Sediment erodability in sediment transport modelling: can we account for biota effects? *Continental Shelf Research* 27, 1116-1142.
- Mathys M (2009). The Quaternary geological evolution of the Belgian Continental Shelf, southern North Sea. PhD Thesis. Universiteit Gent. Faculteit Wetenschappen: Gent. xxiv, pp. 382.
- McCandliss RR, Jones SE, Hearn MR, Latter RJ, Jago CF (2002). Dynamics of suspended particles in coastal waters (southern North Sea) during a spring bloom. *Journal of Sea Research* 47, 285-302.
- Murray JMH, Meadows A, Meadows PS (2002). Biogeochemical implications of microscale interactions between sediment geotechnics and marine benthos: A review. *Geomorphology* 47, 15-30.
- Nechad B, Ruddick KG, Park Y (2010). Calibration and validation of a generic multisensor algorithm for mapping of Total Suspended Matter in turbid waters. *Remote Sensing of Environment* 114, 854-866.
- Nechad B, Van den Eynde D, Fettweis M, Francken F (2003). Suspended particulate matter mapping from multitemporal SeaWiFS imagery over the southern North Sea - SEBAB project, in: Smits, P.C. et al. (Ed.) (2004). *Analysis Of Multi-Temporal Remote Sensing Images: Proceedings Of The Second International Workshop on the Joint Research Centre Ispra, Italy 16-18 July 2003*. pp. 357-367.
- Neukermans G, Ruddick K, Bernard E, Ramon D, Nechad B, Deschamps, P-Y (2009). Mapping total suspended matter from geostationary satellites: a feasibility study with SEVIRI in the Southern North Sea. *Optics Express: the international electronic journal of optics* 17(16), 14029-14052.
- Patt FS, Barnes RA, Eplee RE, Franz BA, Robinson WD (2003). Algorithm updates for the Fourth SeaWiFS data reprocessing, NASA.
- Pietrzak JD, de Boer GJ, Eleveld MA (2011). Mechanisms controlling the intra-annual mesoscale variability of SST and SPM in the southern North Sea. *Continental Shelf Research* 31(6), 594-610.
- Pleskachevsky A, Gayer G, Horstmann J, Rosenthal W (2005). Synergy of satellite remote sensing and numerical modeling for monitoring of suspended particulate matter. *Ocean Dynamics* 55, 2-9.
- Rodriguez-Palma O (2011). The role of suspended particulate matter in the distribution and structure of macrobenthic communities in the Belgian part of the North Sea. MSc Thesis. University Brussels. pp. 56.
- Ruhl CA, Schoellhamer DH, Stumpf RP, Lindsay CL (2001). Combined use of remote sensing and continuous monitoring to analyse the variability of suspended-sediment concentrations in San Francisco Bay, California. *Estuarine, Coastal and Shelf Science* 53, 801-812.
- Schoellhamer DA (2002). Variability of suspended-sediment concentration at tidal to annual time scales in San Francisco Bay, USA. *Continental Shelf Research* 22, 1857-1866.

- Siegismund F, Schrum C (2001). Decadal changes in the wind forcing over the North Sea. *Climate Research* 18, 39-45.
- Sirjacobs D, Alvera Azcárate A, Barth A, Lacroix G, Park Y, Nechad B, Ruddick K, Beckers J-M (2011). Cloud filling of ocean colour and sea surface temperature remote sensing products over the Southern North Sea by the Data Interpolating Empirical Orthogonal Functions methodology. *Journal of Sea Research* 65(1), 114-130.
- Trisakti B, Parwati Budhiman S (2005). Study of MODIS-AQUA data for mapping total suspended matter (TSM) in coastal waters. *Remote Sensing and Earth Sciences* 2, 19-31.
- Ullmann A, Monbalju J (2010). Changes in atmospheric circulation over the North Atlantic and sea surge variations along the Belgian coast during the 20th century. *International Journal of Climatology* 30, 558-568.
- Van Maldegem DC, Mulder HPJ, Langerak A (1993). A cohesive sediment balance for the Scheldt estuary. *Netherlands Journal of Aquatic Ecology* 27 (2-4), 247-256.
- van Raaphorst W, Philippart CJM, Smit JPC, Dijkstra EJ, Malschaert JEP (1998). Distribution of suspended particulate matter in the North Sea as inferred from NOAA/ AVHRR reflectance images and in-situ observations. *Journal of Sea Research* 39, 197-215.
- van der Wal D, Wielemaker-Van den Dool A, Herman P (2010). Spatial synchrony in intertidal benthic algal biomass in temperate coastal and estuarine ecosystems. *Ecosystems* 13, 338-351.
- Van den Eynde D, Nechad B, Fettweis F, Francken F (2007). Seasonal variability of suspended particulate matter observed from SEAWiFS images near the Belgian coast. *Estuarine and Coastal Fine Sediments Dynamics*. In: Maa, JP-Y, Sanford LP, Schoellhamer DH (eds.), *Estuarine and Coastal Fine Sediments Dynamics*. Elsevier, pp. 291-311.
- Van den Eynde D, De Sutter R, De Smet L, Francken F, Haelters J, Maes F, Malfait E, Ozer J, Polet H, Ponsar S, Reijns J, Van der Biest K, Vanderperren E, Verwaest T, Volckaert A, Willekens M (2011). Evaluation of climate change impacts and adaptation responses for marine activities. Final Report - Draft. Brussels : Belgian Science Policy, pp. 114.
- Velegakis AF, Gao S, Lafite R, Dupont JP, Huault MF, Nash LA, Collins MB (1997). Re-suspension and advection processes affecting suspended particulate matter concentrations in the central English Channel. *Journal of Sea Research* 38, 17-34.
- Verfaillie E, Van Lancker V, Van Meirvenne M (2006). Multivariate geostatistics for the predictive modelling of the surficial sand distribution in shelf seas. *Continental Shelf Research* 26(19), 2454-2468.
- Verlaan PAJ, Donze M, Kuik P (1998). Marine vs. fluvial suspended matter in the Scheldt estuary. *Estuarine, Coastal and Shelf Science* 46 (6), 873-883.
- Vos RJ, Gerritsen H (1997). Use of NOAA/AVHRR satellite remote sensing data for modelling of suspended sediment transport in the North Sea: approach in the PROMISE project. WL rapport Z2025, januari 1997. I.o.v. CEC - DGXII – MAST-3.
- Wieringa J, Rijkort PJ (1983). Windklimaat van Nederland. Staatsuitgeverij, Den Haag, pp. 263 (in Dutch).
- Zeelmaekers E (2011). Computerized qualitative and quantitative clay mineralogy: introduction and application to known geological cases. PhD Thesis. Katholieke Universiteit Leuven. Groep Wetenschap en Technologie: Heverlee. ISBN 978-90-8649-414-9. XII, pp. 397.
- Yang L (1998). Modelling of hydrodynamic processes in the Belgian coastal zone. PhD Thesis. Katholieke Universiteit Leuven, Belgium. pp. 214.

